

Effect of magnetic field and boron addition on the structural and magnetic properties of the rapidly solidified $\text{Fe}_{60}\text{Nd}_{35}\text{Al}_5$ master alloys magnet by suction casting

Badis Bendjemil^{1,2,*}, Nassima Seghairi³, Abderrezak Bouchareb^{1,4}, Ali Hafs¹, Marcello Barrico⁴

¹LEREC, University of Badji-Mokhtar, B. P. 12, 23000 Annaba, Algeria

²University of 8 may 1945 Guelma, B. P. 401, 24000 Guelma, Algeria

³University of Oum El-Bouaghi, , B. P. 205, 04000 Oum El-Bouaghi, Algeria

⁴Dip. Chimica I.F.M and INFN/INSTM, Università di Torino, via Giuria 9, 10125 Torino, Italy

Abstract

Ingots with nominal composition $(\text{Nd}_{0.60} \text{Fe}_{0.35} \text{Al}_{0.05})_{100-x} \text{B}_x$ with $x=2$ were produced by arc-melting of elemental Nd, Fe, Al, B and Fe-B alloy with the purity of 99.9% under argon atmosphere. Specimen (dimension: $35 \times 10 \times 10 \text{ mm}^3$) were prepared by suction casting into a copper mold. An influence of the annealing with and without applied magnetic field of a 140 Oe in a furnace with a vacuum of $2 \times 10^{-4} \text{ Pa}$ at 823 K function of annealing time, process was investigated in B-doped Nd-Fe-Al rapidly solidified magnets. The microstructure, structural properties and magnetic domains of the Fe-Nd-Al alloys prepared by suction casting with boron addition have been investigated. The increasing of the annealing time of the sample significantly increases the intrinsic coercivity (iHc) and decreases the proportion of the amorphous phase. The magnetization at the maximum applied field (σ_s) of the Fe-Nd-Al-B alloys decreases, while the coercivity increases markedly after annealing. The high intrinsic coercivity is due to the presence of the $\text{Nd}_2\text{Fe}_{14}\text{B}$ phase. This can be confirmed by the structural, magnetic properties and microstructure using DSC, XRD, VSM, SEM and optical microscopy, in addition the magnetic domains by AFM-MFM.

Keywords: Arc melting, B-doped Nd-Fe-Al type magnets, Phase composition, Structural properties.

PACS: 64.70.dj, 75.30.kz, 68.55Nq, 61.43.Bn.

1. Introduction

The study on the hard magnetic ferrous bulk amorphous alloy date back to the early 1980's when Croat studied several compositions in Nd-Fe and Pr-Fe alloy systems [1]. At the end of the last decade K. Nagayama *et al.* [2] made investigations of the magnetic properties of these alloys. The limiting feature of the production of amorphous alloys is the high critical cooling rate which could be realized by melt spinning method. Therefore, most of the work has been done on ribbons. At that time good soft magnetic properties of these alloys attracted attention as a new type of soft magnetic

*) For correspondence; Email: Badis23@yahoo.fr.

material. In the mid 1990's, on the basis of the empirical rules to achieve high GFA a number of Fe-based alloys have been found with ferromagnetism at room temperature. Recently, it has been found that bulk amorphous alloys are formed in multicomponent Fe-based systems such as Fe-(Al,Ga)-(P,C,B)[3] and Fe,Co/Ni)-(Zr,Hf/Nb)-B[4]. At the same time Inoue and his co-workers discovered another bulk amorphous alloy Nd-Fe-Al with permanent magnetic properties [5]. And finally, the series Fe-Co-Nd-Dy-B came in to being due to Inoue *et al.* [6]

After the discovery of an amorphous phase in hard ferromagnetic alloys in 1996, there has been a growing interest in developing bulk amorphous alloys at moderate cooling rates. Amorphous ferromagnetic alloys in general are not expected to show a high value of coercivity due to lack of magnetocrystalline anisotropy H_a . Hard magnetic properties appear in crystalline materials having a significantly high value of H_a .

The best available hard magnetic materials have lower saturation magnetization J_s than many soft magnetic materials. Due to the presence of a substantial amount of rare earth elements, they are chemically very reactive and also expensive. Therefore attempts are made to produce permanent magnets of composite materials consisting of two suitably dispersed ferromagnetic and mutually exchange-coupled phases, one of which is hard magnetic in order to provide a high coercive field, while the other may be soft magnetic just providing a high saturation magnetization J_s and should envelope the hard phase regions in order to prevent their corrosion. The major application of the present alloy;

- 1) Permanent magnet
- 2) High power electric motors
- 3) Power electronics applications
- 4) Transducer and sensors
- 5) Magnetic levitation and other application of magnet technology.

The hard magnetic properties of the Fe-Co-Ln-B (Ln= Sm, Tb, Dy,Nd) series of alloy with a large supercooled region has been reported earlier [7].

Glass transition and supercooled region were observed in the composition range of 4-56 at% Co, 2-4 at %Nd and 18-30 at % B in melt-spun Fe-Co-Nd-0.5 at% Dy-B amorphous alloys. Presence of Nd in the composition gives rise to $Nd_2Fe_{14}B$ hard magnetic phase, while the presence of a small amount of Dy increases the intrinsic coercivity and also enhances the magnetocrystalline anisotropy of the $Nd_2Fe_{14}B$ phase. The crystallized structure consists of α -Fe, Fe_3B , $Nd_2Fe_{14}B$ and remaining amorphous phase. The formation of this fine mixed structure of crystalline and amorphous phases leads to improved hard magnetic properties resulting from exchange magnetic coupling interaction between the ferromagnetic phases of $Nd_2Fe_{14}B$, Fe_3B , α -Fe and residual amorphous phase owing to a small interparticle spacing.

A multicomponent $Fe_{67}Co_{9.5}Nd_3Dy_{0.5}B_{20}$ alloy is examined because it has the largest supercooled region prior to crystallization in the $Fe_{99.5-x-y-z}Co_xNd_yDy_{0.5}B_z$ system. Several experiments are carried out with the following major objectives.

To obtain the selected alloy in the amorphous ribbon form, melt-spinning experiments are carried out. Thermal analysis is done to explore the thermal stability of the ribbon and also to induce crystallization for the study of the hard magnetic properties of the material.

The amorphous and crystalline phases of this material are examined magnetic properties of the ribbons such as H_c , J_s , B_r are studied by a vibrating sample magnetometer (VSM) under the applied field of 1500 kA/m.

Bulk magnetic properties are studied after consolidating the crushed ribbon. Magnetic and thermal properties are discussed in correlation to the microstructure. The preparation of the $\text{Nd}_{70}\text{Fe}_{20}\text{Al}_{10}$ alloy has attracted much attention due to its high glass-forming ability and hard magnetic behavior at room temperature, but the low saturation magnetization restricts its application [8]. With the addition of Fe, the saturation magnetization becomes much higher, but the glass-forming ability decreases. In the previous work [9], it found that the $\text{Nd}_{70}\text{Fe}_{20}\text{Al}_{10}$ alloy had the high glass-forming ability in the Nd-Fe-Al alloys system. However, it shows soft magnetic behavior at room temperature. This paper report our attempt in improving the glass-forming ability and magnetic and structural properties of the bulk amorphous $\text{Fe}_{60}\text{Nd}_{35}\text{Al}_5$ alloy by addition of boron and annealing time under applied field.

2. Experimental

First of all, master alloys of ternary systems Fe-Nd-Al with composition of 60, 35, 5 % at Fe, Nd and Al with addition of 2 % (B and Fe-B) has been prepared by suction casting into a copper mold (arc melting) of pure elements at our laboratory. Specimen (dimension: $35 \times 10 \times 8 \text{ mm}^3$) were prepared by suction casting into a copper mold. The Master alloys have been prepared from pure elements by arc melting under Ar and He atmosphere.

The ingot was remelted several times in order to obtain a good homogeneity. Melt spinning technique will be used in the future work to obtain ribbons. X-ray diffraction (XRD) (Cu K_α) was performed to examine the structure. The microstructure was studied using optical microscope (OM), scanning electron microscope (SEM) and composition analysis was carried out with EDS. Thermal analysis was performed by differential scanning calorimetry (DSC) at heating rate of 0.33 K/s. In addition we have used the VSM and AFM-MFM to explore the magnetic properties and domains of the $\text{Nd}_2\text{Fe}_{14}\text{B}$ phase after annealing.

3. Results and discussion

Fig. 2 exhibits DSC curves of the of the obtained $(\text{Nd}_{0.60}\text{Fe}_{0.35}\text{Al}_{0.05})_{100-x} \text{B}_x$ with $x=2$ alloy (Fig.1) at a constant heating rate of 0.33 K/s. It can be seen that neither glass transition nor super cooled liquid region before crystallization is observed. An exothermal peak is clearly found corresponding to crystallization for all the samples, indicating that these specimens contain a certain amount of amorphous phase. The heats of crystallization of the main crystallization peak are 6.75 J/g. Furthermore, the onset of the crystallization temperature (T_x) corresponding to the crystallization of the amorphous phase.

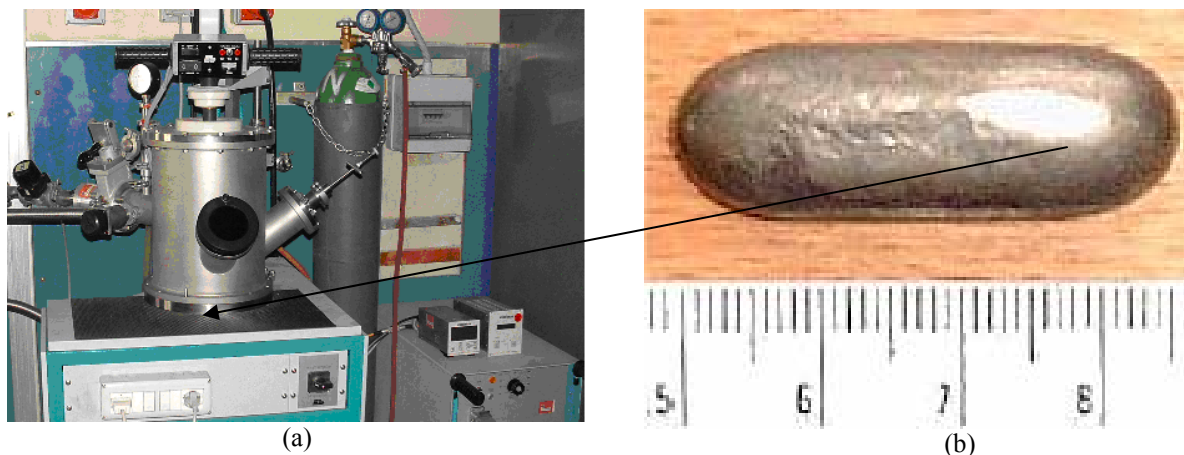


Fig. 1: (a) Arc melting apparatus with suction casting into a copper mold, (b) Bulk sample of the $(\text{Nd}_{0.60}\text{Fe}_{0.35}\text{Al}_{0.05})_{100-x}\text{B}_x$ ($x=2$) produced by suction casting.

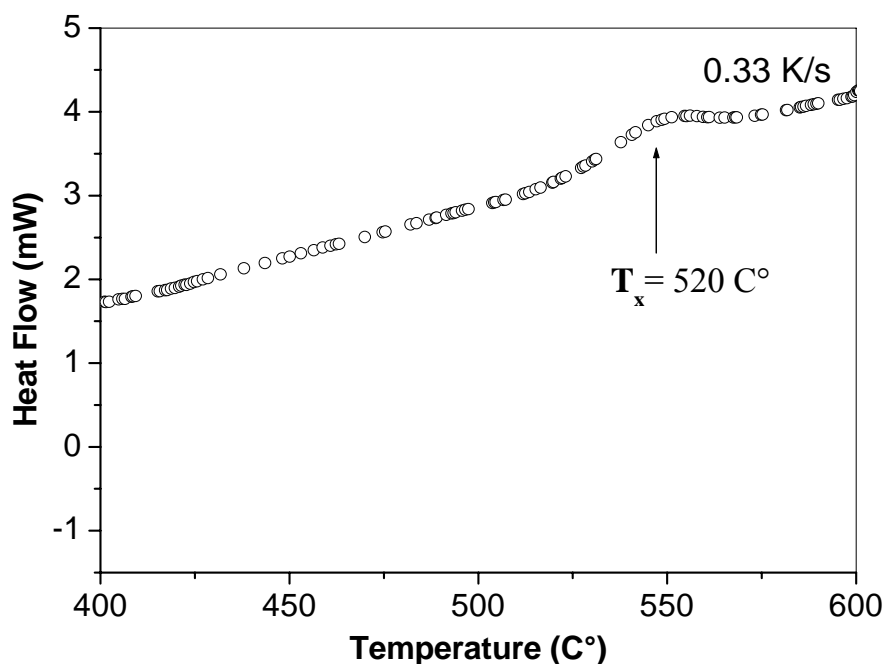


Fig. 2: DSC curves of the $(\text{Nd}_{0.60}\text{Fe}_{0.35}\text{Al}_{0.05})_{100-x}\text{B}_x$ ($x=2$).

From the X-ray diffraction patterns (Fig.3) of the $(\text{Nd}_{0.60}\text{Fe}_{0.35}\text{Al}_{0.05})_{100-x}\text{B}_x$ with $x=2$, the samples are confirmed to be a mixture of amorphous and crystalline phases. Proportion of the amorphous phase decreases with the addition of boron and annealing time (1, 2, 3h) at $T=550^{\circ}\text{C}$.

At the annealing temperature 550°C during 1h a broad high intensity peak around $2\theta = 50^{\circ}$ appears is increased, which corresponds to $\alpha\text{-Fe}$ besides other weak crystalline peaks corresponding to Fe_3B , Fe_2B and FeB crystalline phases can be detected.

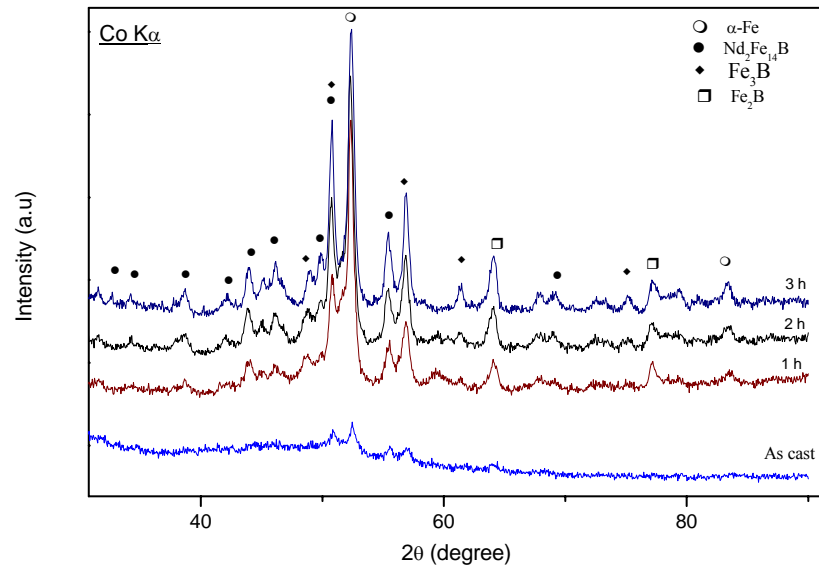
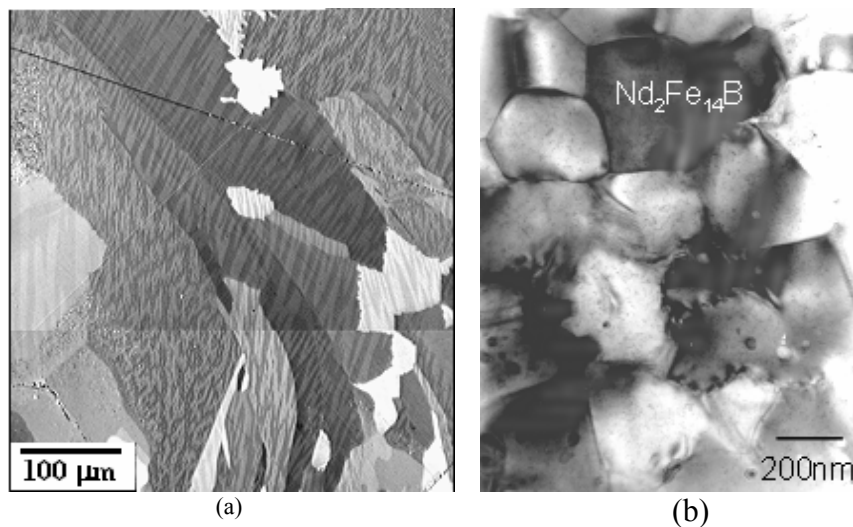


Fig. 3: X-ray diffraction patterns of as cast $(\text{Nd}_{0.60}\text{Fe}_{0.35}\text{Al}_{0.05})_{100-x}\text{B}_x$ ($x=2$) and annealed at $T=550\text{ C}^\circ$ with different annealing times under high magnetic field.

With the increase of the annealing time the broad peak at 1 h develops into a sharp peak at $2\theta = 52^\circ$ corresponding to $\alpha\text{-Fe}$ and a peak slightly developing at $2\theta = 51^\circ$. The peak at $2\theta = 51^\circ$ gradually becomes prominent with increasing temperature and corresponds to Fe_3B and $\text{Nd}_2\text{Fe}_{14}\text{B}$. The peak corresponding to the equilibrium phase Fe_2B appears at $2\theta = 56^\circ$ and $2\theta = 64^\circ$ (Fig. 3). From the XRD patterns it is revealed that the microstructure changes from completely amorphous to amorphous and crystalline and finally to completely crystalline. This result is also corroborated by TEM image and thermal studies (discussed in Fig 4 and 3).



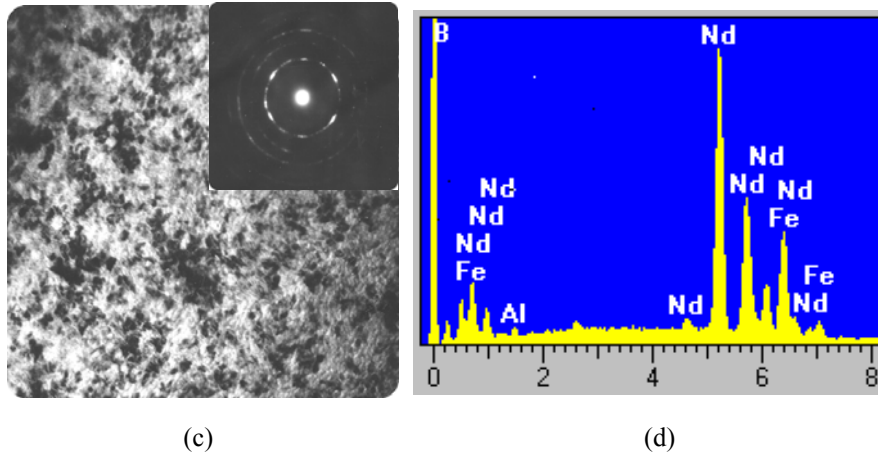


Fig. 4: (a, b) OM and SEM pictures of the bulk sample $(\text{Nd}_{0.60}\text{Fe}_{0.35}\text{Al}_{0.05})_{100-x}\text{B}_x$ ($x=2$), (c, d) TEM picture with ED and EDS spectra after annealing of $\text{Nd}_2\text{Fe}_{14}\text{B}$ phase is highlighted.

This is confirmed by the SEM, OM pictures (before annealing) and EDS analysis TEM picture of this sample (after annealing) shows stripped regions of $\text{Nd}_2\text{Fe}_{14}\text{B}$ phase (marked by arrow) (Fig.4).

The $\text{Nd}_2\text{Fe}_{14}\text{B}$ phase appears, and the diffraction peak intensity of the $\text{Nd}_2\text{Fe}_{14}\text{B}$ phase increases with increasing the annealing time according (Fig.3), indicating that the volume fraction of the $\text{Nd}_2\text{Fe}_{14}\text{B}$ phase increases. The appearance and increase of the $\text{Nd}_2\text{Fe}_{14}\text{B}$ phase are the reasons for the change of magnetic behavior and the increasing intrinsic coercivity of the alloys after optimal annealing time (3 h) (Fig.5). This is demonstrated in the microstructure of the magnetic domains using magnetic force microscope coupled with atomic force microscope AFM-MFM (Fig.6).

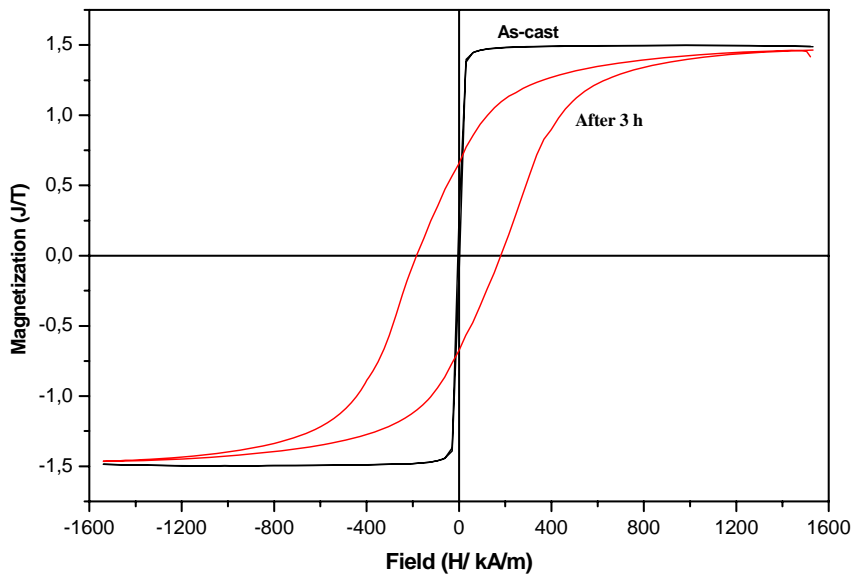


Fig.5: Hysteresis loop (VSM) curves of the as cast bulk sample $(\text{Nd}_{0.60}\text{Fe}_{0.35}\text{Al}_{0.05})_{100-x}\text{B}_x$ ($x=2$) and annealed at $T=550\text{ }^\circ\text{C}$ during 3 h.

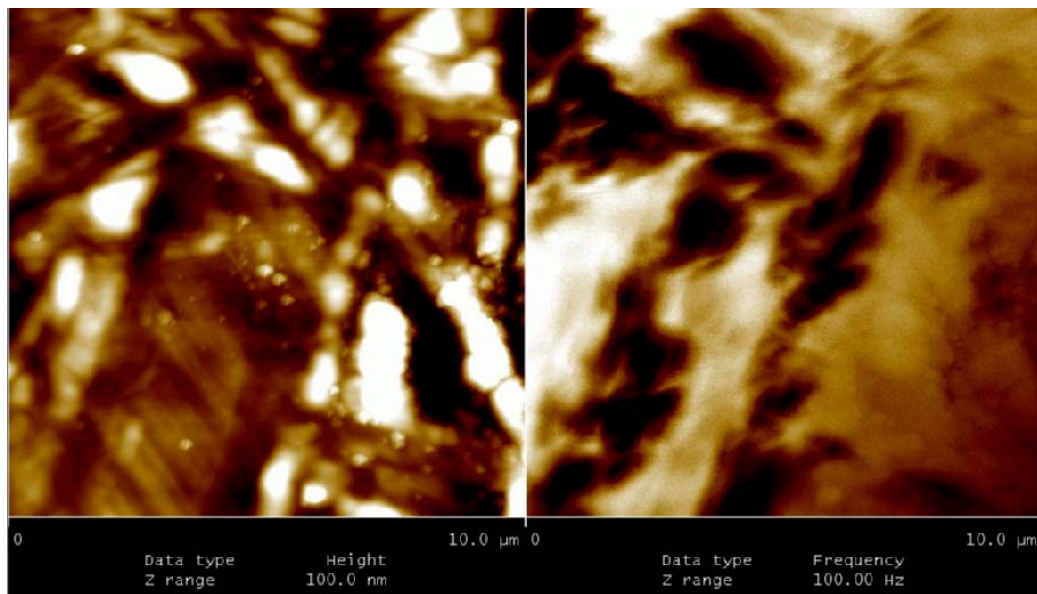


Fig.6: AFM-MFM pictures of the magnetic domains in the bulk sample $(\text{Nd}_{0.60}\text{Fe}_{0.35}\text{Al}_{0.05})_{100-x}\text{B}_x$ ($x=2$) annealed at 550°C during 3h, the magnetic domains of the $\text{Nd}_2\text{Fe}_{14}\text{B}$ phase is highlighted.

4. Summary

The annealing time with addition of boron in Fe-Nd-Al alloy significantly increases the intrinsic coercivity and decreases the proportion of the amorphous phase. The magnetization at the maximum applied field of the Fe-Nd-Al-B alloys decreases, while the coercivity increases markedly after annealing time. The high intrinsic coercivity is due to the presence of the $\text{Nd}_2\text{Fe}_{14}\text{B}$ phase. The magnetic field applied favors the orientation of the $\text{Nd}_2\text{Fe}_{14}\text{B}$ phase at the preferential axis *c* in the matrix.

Acknowledgements

We acknowledge the group of Prof. M. Barrico for the synthesis of the samples and OM, SEM pictures, XRD and EDS analysis. The group of the Prof. F. Vinai (INRIM-Torino): Drs P. Tiberto, E. Ferrara, F. Selegato and M. Coisson and their technical assistance for the help in the sample annealing (high magnetic field and high vacuum furnace, and DSC and AFM-MFM characterisations).

References

- [1] K. Sirator, K. Nagayama, *Appl. Phys. Lett.* **70** (1999) 1763
- [2] K. Toshiyuki, N. Katsuhisa, U. Takateru, *J. Magnetism and Magnetic Mater.* **117** (1997) 379
- [3] A. Inoue, A. Murakami, T. Zhang, A. Takeuchi, *Mater. Trans. JIM* **39** (1997) 205
- [4] I. T. Zhang, T. Masumoto, *Mater. Trans. JIM* **30** (1989) 965
- [5] I. T. Zhang, W. Zhang, A. Takeuchi, *Materials T. JIM* **37** (1996) 99

- [6] I. T. Zhang, W. Zhang, A. Takeuchi, Mater. T. JIM **37** (1996) 99
- [7] I. T. Zhang, T. Masumoto, Mater. T. JIM **30** (1999) 522
- [8] E. Olivetti, M. Baricco, E. Ferrara, P. Tiberto, L. Martini, J. Magnetism and Magnetic Mater. (2005) 1214
- [9] E. Olivetti, E. Ferrara, P. Tiberto, M. Baricco, J. Magnetism and Magnetic Mater. (2004) 1949